Structural Engineering and Mechanics, Vol. 40, No. 6 (2011) 745-762 745
DOI: http://dx.doi.org/10.12989/sem.2011.40.6.745

Signal processing based damage detection in structures subjected to random excitations

Luis A. Montejo*

Department of Engineering Science and Materials, University of Puerto Rico at Mayagüez, Mayagüez, Puerto Rico

(Received September 13, 2010, Revised April 7, 2011, Accepted October 12, 2011)

Abstract. Damage detection methodologies based on the direct examination of the nonlinear-nonstationary characteristics of the structure dynamic response may play an important role in online structural health monitoring applications. Different signal processing based damage detection methodologies have been proposed based on the uncovering of spikes in the high frequency component of the structural response obtained via Discrete Wavelet transforms, Hilbert-Huang transforms or high pass filtering. The performance of these approaches in systems subjected to different types of excitation is evaluated in this paper. It is found that in the case of random excitations, like earthquake accelerations, the effectiveness of such methodologies is limited. An alternative damage detection approach using the Continuous Wavelet Transform (CWT) is also evaluated to overcome this limitation. Using the CWT has the advantage that the central frequencies at which it operates can be defined by the user while the frequency bands of the detail functions obtained via DWT are predetermined by the sampling period of the signal.

Keywords: damage detection; wavelet transform; empirical mode decomposition; butterworth filters; hilbert transform

1. Introduction

Although visual or localized experimental damage-detection methods (e.g., acoustic, ultrasonic, magnetic or thermal methods) are capable of identifying and determining the extent of damage, effective application of all of these techniques require previous knowledge of the damage vicinity and the portion of the structure under inspection to be easily reached (Doebling *et al*. 1998). Moreover, a comprehensive application of localized damage detection methods to a complex structure is a lengthy and expensive assignment. An inspection of the Golden Gate Bridge main cables, anchorages and tie-downs was performed at a cost of $226,900 in 1998 (Sohn *et al*. 2003). Visual inspections after the M6.3 Abruzzo earthquake (Italy, April 6, 2009) lasted more than 4 months and deployed about 1500 inspectors daily (EERI 2009).

The aforementioned localized damage detection methods limitations have been one of the main motivations for the continuous research and development of quantitative global damage-detection methods. Damage identification based upon changes in vibration characteristics has been the preferred approach to monitor changes in the structure on a global basis. Vibration based damage detection

*Corresponding author, Assistant Professor, E-mail: luis.montejo@upr.edu

(VBDD) fundamental principle is that changes in the physical properties of the structure (mass, energy dissipation mechanisms and stiffness) will cause changes on the modal parameters (frequencies, mode shapes, and modal damping). Detailed literature reviews concerning these techniques and response parameters used for damage identification can be found elsewhere (Doebling *et al*. 1996, Farrar and Doebling 2001, Sohn *et al*. 2003).

Despite the apparently intuitive nature of VBDD, different researchers and practitioners have found significant technical challenges: (1) In order to avoid premature collapse modern civil structures are designed to be highly redundant, therefore the occurrence of damage (which is typically a local phenomenon) may not significantly influence global response of a structure (Farrar and Doebling 2001, Farrar and Cone 1995). (2) Since structural damage is usually reflected in the high frequency response of the structure, methods that monitor changes in the shape modes require a large spatial resolution in the sensor network in order to capture high order modes. Such a dense sensor network array is not usually available in complex civil structures. (3) Some of the available methodologies largely depend on the updating of a detailed finite element (FE) model. Due to large computational demands and difficulties involved in obtaining the FE model, this approach may become unfeasible for complex structures (Rodgers and Çelebi 2006). (4) Many algorithms presume that a data set from the undamaged structure is available and the damage detection is performed by comparison of the dynamic response characteristics of the pristine and damaged structures. This type of approaches has the inconvenient that the events that occurred between dynamic measures are lost and significant information can be missed. Todorovska and Trifunac (2007) investigated the frequency variations during the 1979 Imperial Valley earthquake of a six-story reinforced concrete structure that was severely damaged by the earthquake. They detected a decrease in the system frequency of about 44% that can be attributed to structural damage followed by a 35% increase at the end of the recorded shaking. Notice that in this case the severity of damage would be underestimated if the damage assessment was to be performed based only on the vibration characteristics of the structure before and after the earthquake. (5) Civil structures are in continuous interaction with the soil they are founded on and with the environment. Experimental results have shown that the changes in vibration properties as a result of such interactions can be of larger proportions than the changes induced in the early stages of damage (Huth *et al*. 2005, Clinton *et al*. 2006).

In order to overcome the issues of conventional VBDD methodologies some authors have explored the possibility of identifying damage from the direct examination of the nonlinear-nonstationary characteristics of the dynamic response, eliminating in this way the dependency on large and detailed FE models or on the prior knowledge of the undamaged structure vibration characteristics. Analysis of the registered structural response is performed using high pass filtering or signal processing tools that allow for simultaneous time frequency examination, e.g. Wavelets (Mallat 1989) and Hilbert-Huang transforms (Huang *et al*. 1998). The occurrence of damage is associated with any changes in the vibration parameters (instantaneous frequency or damping) or with the occurrence of singularities in the high frequency response. This paper focuses on the second alternative, i.e. the detection of singularities (novelties or spikes) in the high frequency component of the structural response. Investigations on the parameter identification capabilities of these transforms are available elsewhere (Kijewski and Kareem 2003, Yang *et al*. 2004, Yan and Miyamoto 2006, Kijewski-Correa and Kareem 2006). In addition, methodologies that rely on measuring wave travel times using impulse response functions computed by deconvolution of each floor dynamic response are also under development (Todorovska 2009).

2. Simultaneous time-frequency analysis

A time-frequency analysis of a signal can provide information about how the frequency content of the signal evolves with time, thus providing a tool to dissect and interpret strongly non-stationary signals. Methods like the Short Time Fourier transform allow for the construction of a time-frequency map of the signal, however, its constant resolution time-frequency window is not suitable for detecting certain phenomena out of the resolution of the window. More recently developed methodologies like Wavelet and Hilbert Huang transforms were devised to overcome these limitations. These methods are able to provide information about the slow varying phenomena of a signal and at the same time, permit the detection of sudden discontinuities.

2.1 Wavelet transforms

As with the Fourier transform, there are two types of wavelet transform: the continuous and discrete version. The Continuous Wavelet Transform (CWT) takes a function $x(t)$ of a real variable and transforms it to a function $C(s, p)$ of two real variables s and p

$$C(s, p) = \int_{-\infty}^{\infty} x(t)\psi_{s,p}(t)dt \tag{1}$$

The wavelet coefficients $C(s, p)$ contain information about the function $x(t)$ at the scale s around the time position p. The functions $\psi_{s,p}(t)$ are defined by translating along the time axis and stretching or compressing a "mother wavelet" $\Psi(t)$

$$\psi_{s,p}(t) = \frac{1}{\sqrt{s}}\Psi\left(\frac{t-p}{s}\right) \tag{2}$$

In order to recover the original signal $f(t)$ it is necessary to use the "reconstruction formula"

$$x(t) = \frac{1}{K_\psi}\int_{s=0}^{\infty}\left(\int_{p=-\infty}^{\infty} C(s, p)\psi_{s,p}(t)\frac{dp}{s^2}\right)ds = \frac{1}{K_\psi}\int_0^{\infty} D(s, t)ds \tag{3}$$

where K_ψ is a constant that depends on the mother wavelet. The functions within parenthesis in Eq. (3) are referred to as the "detail functions" $D(s,t)$ and have a dominant frequency that depends on the type of wavelet. In the CWT the wavelet coefficients are calculated at scale values that vary continuously, the result is a highly redundant and time demanding representation of the signal. In the Discrete Wavelet Transform (DWT) the values of scale and position are choose based on a dyadic scale, for some special mother wavelets $\psi(t)$ the corresponding discretized wavelets $\psi_{s,p}(t)$ constitute an orthonormal basis. Mallat (1989) developed a fast wavelet decomposition and reconstruction algorithm for the DWT using a two-channel subband coder. In the DWT, a signal can be represented (Eq. 4) by its approximations (A) and details (D) at different levels of decomposition (j). The approximations are the high-scale, low-frequency components of the signal. The details are the low-scale, high-frequency components.

$$x(t) = A_j + \sum_{i \le j} D_i \tag{4}$$

To demonstrate the application of the wavelet transforms, the signal displayed in Fig. 1(a) was

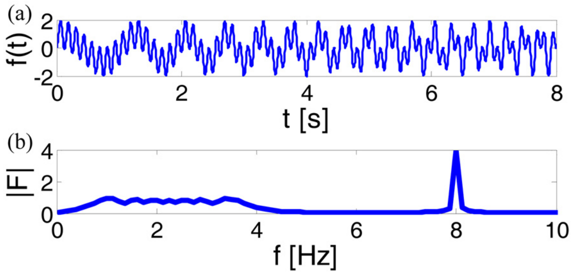

Fig. 1 (a) Signal in the time domain and (b) its Fourier spectrum

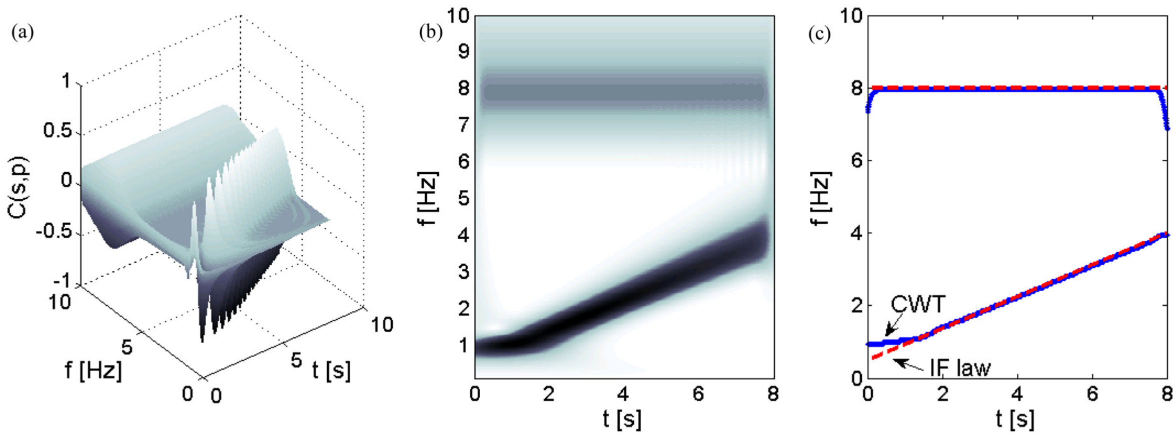

Fig. 2 (a) 3D plot of the wavelet coefficients, (b) wavelet map and (c) instantaneous frequencies from wavelet ridges

artificially generated as the sum of a sinusoidal of frequency 8 Hz and a chirp signal starting with a frequency of 0.5 Hz and increasing linearly up to a frequency of 4 Hz at time 8 seconds. At time 4 seconds a small discontinuity is introduced by multiplying the signal amplitude at that point by 0.99. The Fourier spectrum of the signal is presented in Fig. 1b, it is seen that the Fourier spectrum captured the correct range of frequencies of the signal, but the evolution in time of the frequency content is missed. An analysis in the time-frequency domain using the CWT, shown in Fig. 2, allows us to identify the time where each event took place. Fig. 2(a) shows the real values of the coefficients *C(s,p)* that result from the application of the CWT (Eq. (1)) using the Complex Morlet Wavelet (Eq. (5)). The Morlet Wavelet is essentially a sinusoid modulated by a Gaussian envelope offering optimal resolution in both the time and frequency domain. Fig. 2(b) is similar to Fig. 2(a), but now the wavelet coefficients *C(s,p)* are shown in a two-dimensional graph with their absolute values plotted. This is the usual form to graph the coefficients and it is called a Wavelet Map. The darker colors indicate higher values of the wavelet coefficients. By observing the darker colors in the graph, one can perceive the frequency content of the signal at any time instant. A more precise estimation of the instantaneous dominant frequencies can be obtained by identifying each component by a distinct ridge in the time-frequency plane. There are several techniques to identify these ridges (Carmona *et al*. 1997, Todorovska 2001); the instantaneous dominant frequencies in Fig. 2(c) were

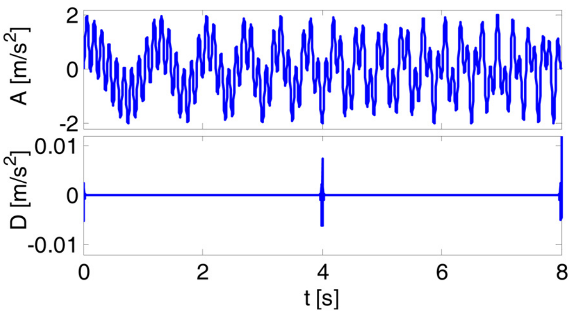

Fig. 3 Approximation (*A*) and detail (*D*) functions at the first level of decomposition via DWT

obtained by locating the local maximas at each time instant. It is seen that the dominant frequencies and its evolution in time are successfully identified for most part of the signal. However, a deviation in the identified instant frequencies (IF) is noticed at the beginning and end of the signal due to the end effects. Different methodologies haven proposed to meliorate the end effects in the CWT, e.g., padding the beginning and end of the signal with surrogate values (Kijewski and Kareem 2003). The results displayed in Fig. 2 were obtained from the original signal without padding.

$$\psi(t) = e^{i2\pi f_0} e^{-t^2/2\sigma^2} \tag{5}$$

If well the frequency content evolution of the signal was properly captured by the CWT analysis, the discontinuity at 4 seconds was not detected. This is because small discontinuities are usually reflected in the high frequency range and the analysis performed was limited to the range 0-10 Hz. One may extend the frequency range over which the CWT is performed until traces of the discontinuity are detected, however this is computationally expensive and the preferred approach is the decomposition of the signal in details and approximations via DWT (Eq. (4)). Note that the Morlet wavelet does not comply with the orthogonality requirements to perform a DWT analysis; therefore the DWT was implemented using the Biorthogonal (Bior) 6.8 basis. The Biorthogonal wavelets are compactly supported biorthogonal spline wavelets for which symmetry and exact reconstruction are possible. Moreover, the Bior 6.8 has been successfully used in the past to uncover discontinuities (Ovanesova and Suarez 2004, Todorovska and Trifunac 2010). Contrary to the Morlet wavelet, Bior wavelets do not have an explicit expression for the wavelet function. The results for the first level decomposition are displayed in Fig. 3. The figure on top shows the low frequency component of the signal, i.e., the approximation function (*A*), and the figure on the bottom shows the high frequency component, i.e., the detail function (*D*). It is seen that the discontinuity in the signal can be associated with the spike at 4 seconds in the detail function.

2.2 Hilbert-Huang Transform

The instantaneous frequency (IF) of a monocomponent signal (i.e., signals in which only one frequency is present at a given time) can be calculated using the Hilbert transform, through which the complex conjugate *y(t)* of the real valued function *x(t)* can be determined by

$$H[x(t)] = \frac{P}{\pi}\int_{-\infty}^{\infty}\frac{x(s)}{t-s}ds \tag{6}$$

where P is the Cauchy principle value. With the Hilbert Transform, the analytic signal is defined as

$$z(t) = x(t) + iH[x(t)] = x(t) + iy(t) = a(t)e^{i\theta(t)} \tag{7}$$

where

$$a(t) = \sqrt{x^2 + y^2} \text{ and } \theta(t) = \arctan(y/x) \tag{8}$$

Here $a(t)$ is the instantaneous amplitude and θ is the phase function. From the definition in Eq. (7), the concept of IF is defined as the time-varying derivative of the phase (θ)

$$f(t) = \frac{1}{2\pi}\frac{d}{dt}\theta(t) \tag{9}$$

It must be noticed that the HT cannot be directly applied to multi-component signals (i.e., signals in which more than a frequency is present at a given time), as the result will be only one (average) instant frequency. To successfully apply the HT to multicomponent signals, the signal needs to be preprocessed into their monocomponent elements (e.g., by bandpass filtering) before implementation of the transform. Huang *et al*. (1998) introduced the concept of Empirical Mode Decomposition (EMD) as an alternative way to separate multicomponent signals into their monocomponent constituents through a progressive sifting process to yield empirical bases termed intrinsic mode functions (IMF). These IMFs are defined so as to ensure that they have well-behaved HTs and conform to a narrowband condition. An IMF represents a simple oscillatory mode as a counterpart to the simple harmonic function, but it is much more general: instead of having a constant amplitude and frequency, as in a simple harmonic component, the IMF can have a variable amplitude and frequency as function of time (Huang 2005). The combination of the EMD and the Hilbert spectral analysis is known as the Hilbert-Huang transform (HHT). Fig. 4 (left) show the first two IMF's obtained after the EMD is applied to the signal previously presented in Fig. 1(a). The instant frequencies in Fig. 4 (right) are obtained by applying the HT to each IMF component. It is seen that for this case the resolution capabilities of the HHT are comparable to the CWT and the signal discontinuity can be identified by the spike at 4 seconds in the instant frequency of the first IMF. The algorithm used in this work to calculate the HHTs is the one provided in Rilling *et al*. (2003).

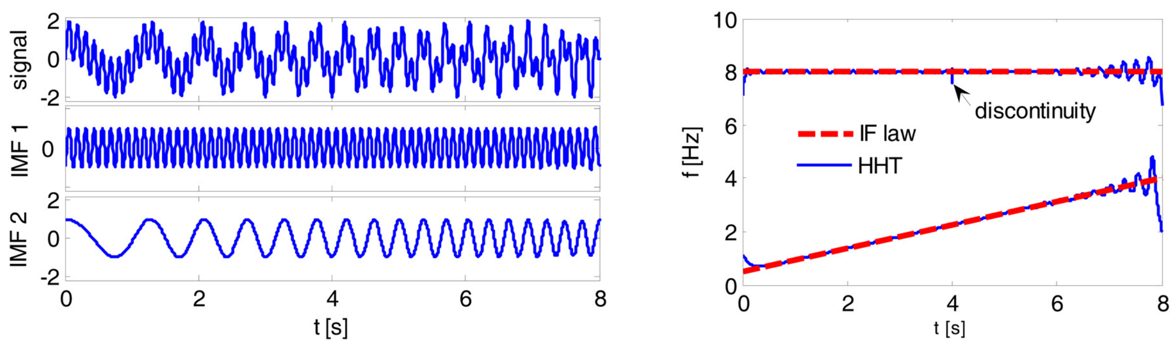

Fig. 4 Intrinsic mode function IMFs (left) and instantaneous frequency via HT (right)

3. Damage detection using signal processing methods

A three storey shear building model (Fig. 5) is used to demonstrate how signal processing has been used to detect structural damage. Natural frequencies of the undamaged building are 2.50 Hz, 6.90 Hz and 9.74 Hz; damping ratio is specified as 5% for all three modes. The structural response is obtained by direct integration using the average acceleration method. Damage is induced at three different times (1/4, 1/2 and 3/4 of the excitation duration) as sudden relative reductions of 5%, 10% and 20% of the 1st floor stiffness (Fig. 5). The resulting changes in the structure natural frequencies are shown in Table 1. It is seen that the reduction in the structure first mode vibration frequency caused by the induced damages is small (between 1% and 10%), the first floor stiffness reduction values used can then be associated with damage related with a local mechanism/member not affecting much the global behavior. Fig. 6 shows the acceleration time histories at each level of the structure when a 3 Hz constant amplitude sinusoidal acceleration is applied at the base, sampling

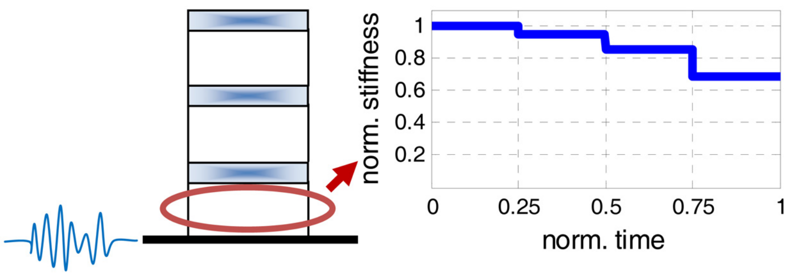

Fig. 5 Shear building model with base excitation and induced damage in the 1st floor

Table 1 Natural frequencies change with induced damages

No damage	Damage 1 (5%)	Damage 2 (10%)	Damage 3 (20%)
2.50 Hz	2.47 Hz	2.40 Hz	2.26 Hz
6.90 Hz	6.84 Hz	6.71 Hz	6.47 Hz
9.74 Hz	9.71 Hz	9.64 Hz	9.54 Hz

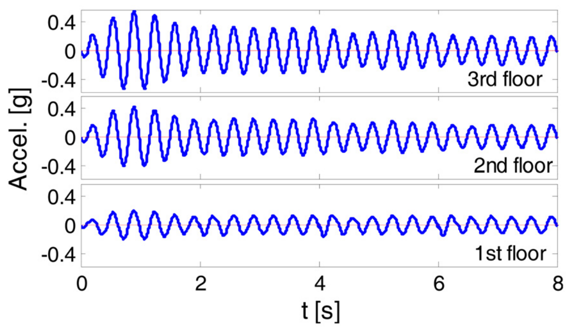

Fig. 6 Acceleration response when a 3Hz constant amplitude sinusoidal acceleration is applied at the base

frequency is 200 Hz. Notice that the induced damages are not evident from a simple inspection of the response. Several researchers (Sone *et al*. 1995, Al-Khalidy *et al*. 1997, Hou and Noori 1995, Todorovska and Trifunac 2010) have noticed that the occurrence of spikes in the DWT high frequency components of the dynamic response coincides with the instant at which damage occurred. Fig. 7 shows the absolute values of the detail functions (high frequency components, Eq. (4)) obtained via DWT with the Bior6.8 wavelet basis for the acceleration response at each level of the structure in Fig. 5. The spikes in the detail functions correspond to the time instants where the damage was induced. Although damage was induced in the 1st floor only, it can be detected from the acceleration histories in any of the floors. Furthermore, the spikes amplitude tends to be related to the relative proximity to the damage location and the amount of damage induced, i.e. the larger spikes are detected from the acceleration on the first floor and for the third damage event at 6 seconds.

The high frequency component (first IMF) obtained after an EMD may also depict localized discontinuities in the structural response (Vincent *et al*. 1999). Fig. 8 shows the first IMF and its IF via HT for each of the levels of the structure in Fig. 5. The two largest induced damages can be detected by the spikes appearing in the IF of the first IMF at the first floor; however the detection of damage instants using the accelerations in the 2nd and 3rd floors is not as clear as with the DWT approach (Fig. 7). Other authors (Yang *et al*. 2004, Xu and Chen 2004) have proposed a different

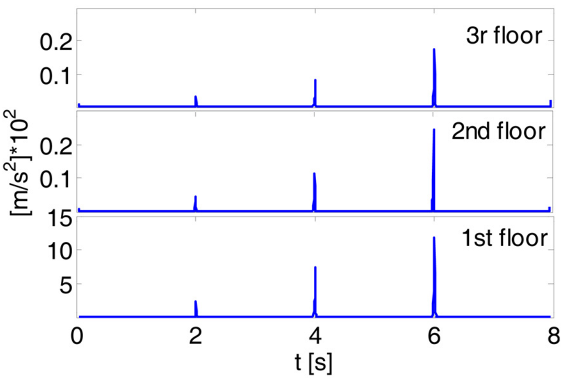

Fig. 7 First level decomposition detail functions (in absolute values) via DWT using Bior6.8 basis

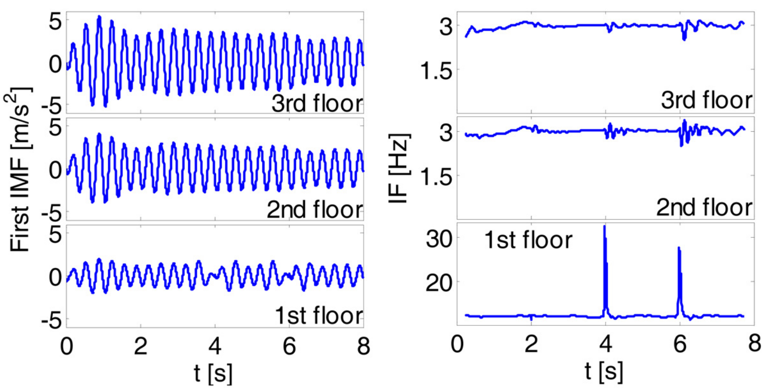

Fig. 8 First IMF (left) and its IF via HT (right) for each of the levels of the structure in Fig. 5

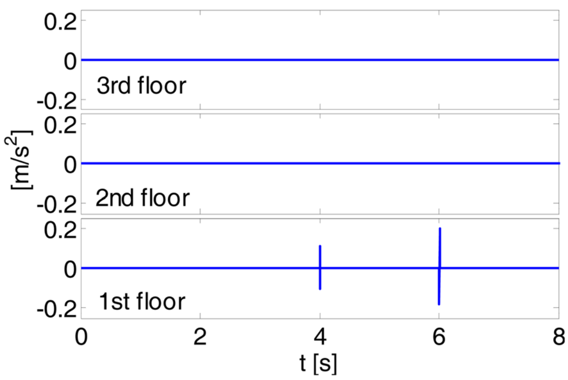

Fig. 9 First IMFs after an intermittency check at 10 Hz

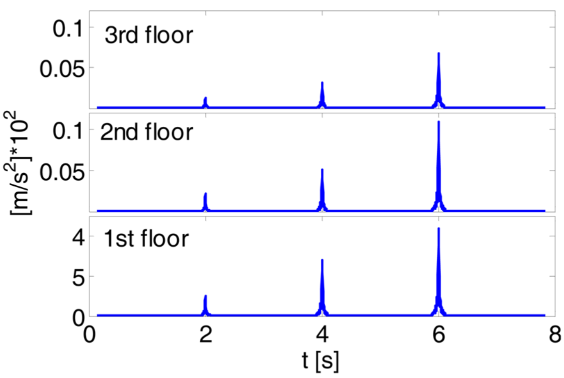

Fig. 10 Floor accelerations (in absolute values) after a 75 Hz high pass filter is applied

approach to use the first IMF resulting from the EMD to detect the occurrence of damage, instead of applying the HT to detect the discontinuities, they post process the first IMF with an intermittency check (Huang *et al.* 1999). In the intermittency check, data from the first IMF having frequencies lower than a specified intermittency frequency is removed by a straightforward counting process. The intermittency frequency should be smaller than the frequency of the discontinuity but larger than the highest structural frequency. The results obtained after applying an intermittency check at 10 Hz to the IMFs in Fig. 8 are displayed in Fig. 9, it is seen that damage instants can be identified from the spikes appearing in the first floor for the two largest damages induced only – no spikes appear in the other floors. Finally, Bisht (2005) observed that a direct high pass filtering of the measured response without any IMF separation can be as effective as any other approach for detecting sudden changes in the system. Fig. 10 shows the acceleration in each of the floors after a 10th order Butterworth high-pass filter to suppress frequencies below 75 Hz is applied, the results obtained are similar to the obtained using the DWT (Fig. 7).

4. Damage detection in structures subjected to random excitations

In order to evaluate the damage detection capabilities of the previously discussed methodologies when the structure is subjected to random excitations, the structure is now subjected to the four acceleration histories shown in Fig. 11 along with their Fourier spectra. The input signals were selected to study the influence of different frequency contents and non-stationary characteristics in the results of the detection methodologies. The first two signals (Fig. 11(a) and 11(b)) are artificially generated white noises that have been passed through low pass filters at 25 Hz and 40 Hz; we will refer to these excitations as wnoise25 and wnoise40, respectively. The other two signals are earthquake acceleration records. The first accelerogram (Fig. 11(c)) was recorded at the Treasure Island station during the M6.93 1980 Loma Prieta earthquake. The second accelerogram (Fig. 11(d)) was recorded at the Mcgee Creek station during the M5.82 1984 Round Valley earthquake. Notice from the Fourier spectra in Fig. 11 that the Round Valley record has a quite spread frequency content compared to the very narrow Fourier spectrum of the Loma Prieta record. Both records were obtained from the NGA database (PEER 2010). All four acceleration histories have a sampling

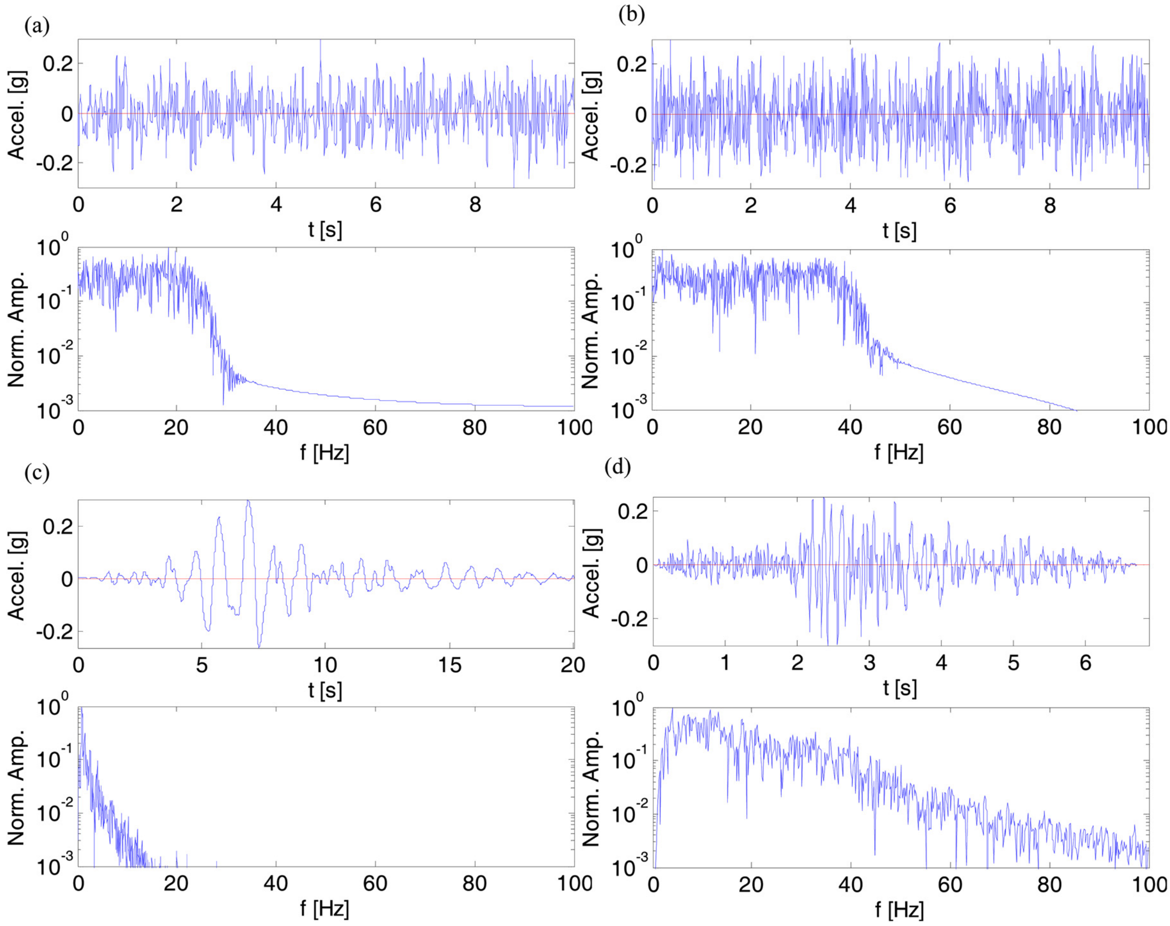

Fig. 11 Four random excitations and its frequency content via Fourier spectrum: (a) white noise HP 25 Hz; (b) White noise HP 40Hz; (c) 1989 Loma Prieta earthquake; (d) 1984 Round Valley earthquake

frequency of 200 Hz and were normalized to a maximum acceleration of 0.3 g.

In the case of the white noise excitations (Figs. 12 and 13), it is seen that the most effective methodology is the high pass filtering at 90 Hz (Figs. 12(d) and 13(d)) since it was able to detect all three damage instants (at 2.5, 5 and 7.5 seconds) from the accelerations at all three levels of the structure. The DWT approach was only successful detecting damage episodes from the first floor acceleration when the building is excited by wnoise25 (Fig. 12(a)). A large amount of spikes appear in the 2nd and 3rd floor (Fig. 12(a)) for wnoise25 and at all levels for wnoise40 (Fig. 13(a)) that are not related with the induced damages. The methodology based on the IF of the first IMF was not able to detect any damage (Figs. 12(b) and 13(b)). The EMD methodology with an intermittency check at 100 Hz was able to detect the first induced damage from the first floor accelerations when wnoise40 is applied (Fig. 13(c)), but did not detected any damage from the accelerations at the other two levels of the structure. In the case of wnoise25 no spikes appear after the intermittency check (Fig. 12(c)).

Fig. 14 show the results obtained when the structure is excited with the Loma Prieta record. None

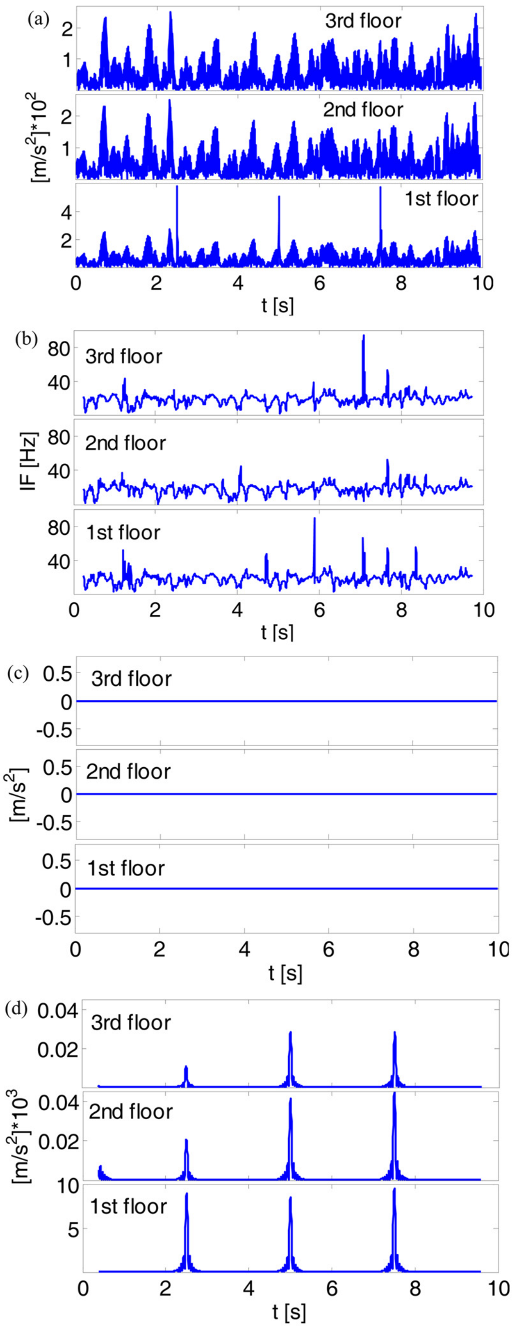

Fig. 12 Damage detection when the structure is exited by white noise HP 25 Hz: (a) First level detail functions (in absolute values) via DWT, (b) IF of the first IMF via HT, (c) IMF 1 with intermittency check at 100 Hz and (d) floor accelerations (in absolute values) after a 90 Hz high pass filter is applied

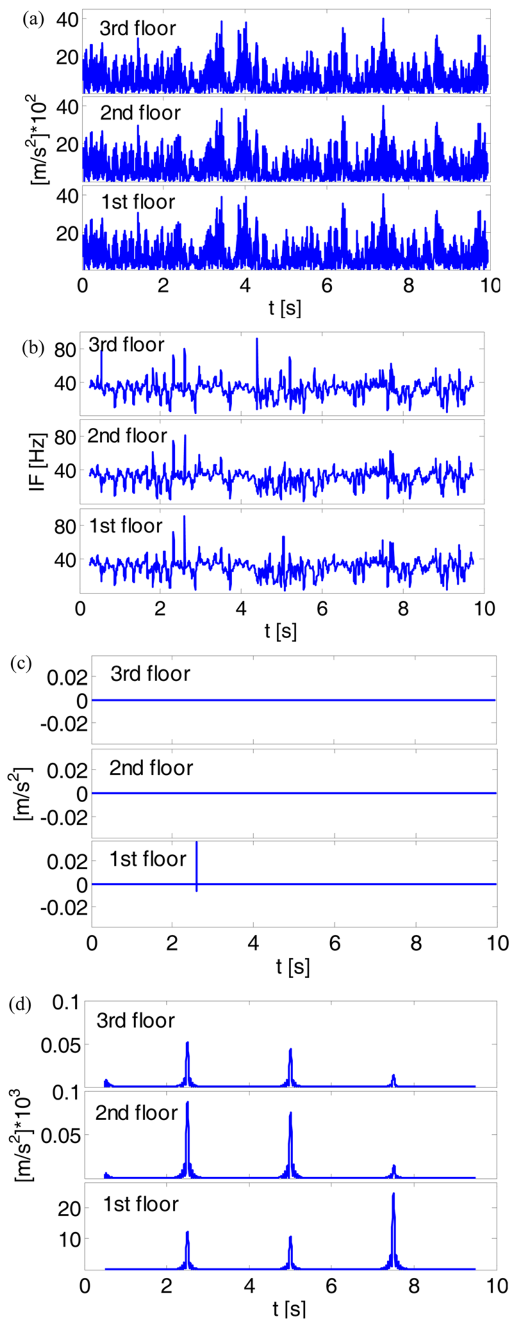

Fig. 13 Damage detection when the structure is exited by white noise HP 40 Hz: (a) First level detail functions (in absolute values) via DWT, (b) IF of the first IMF via HT, (c) IMF 1 with intermittency check at 100 Hz and (d) floor accelerations (in absolute values) after a 90 Hz high pass filter is applied

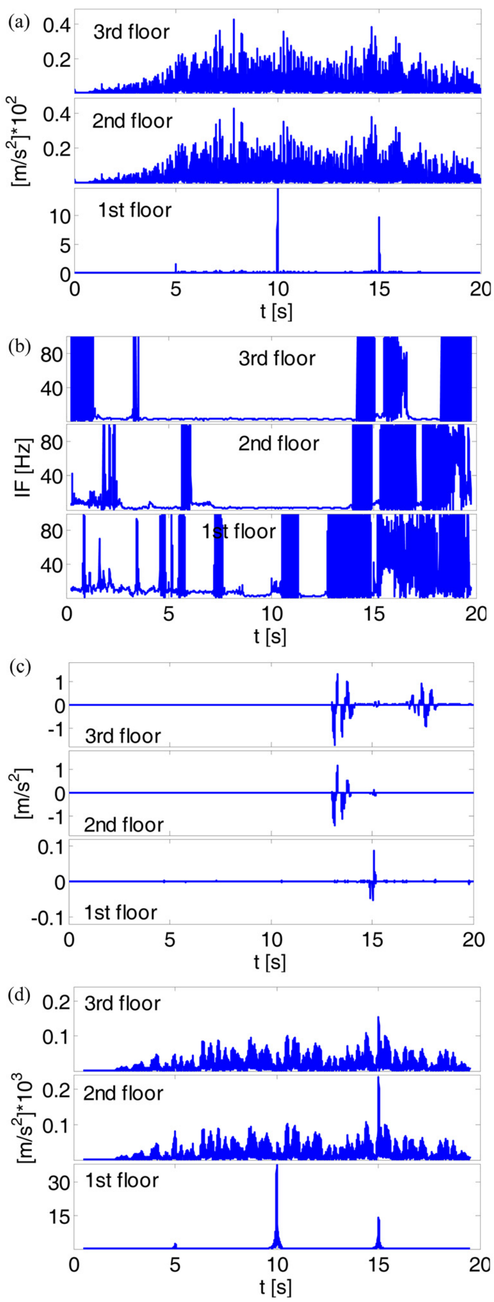

Fig. 14 Damage detection when the structure is exited by an acceleration record from the 1989 Loma Prieta earthquake: (a) First level detail functions (in absolute values) via DWT, (b) IF of the first IMF via HT, (c) IMF 1 with intermittency check at 100 Hz and (d) floor accelerations (in absolute values) after a 90 Hz high pass filter is applied

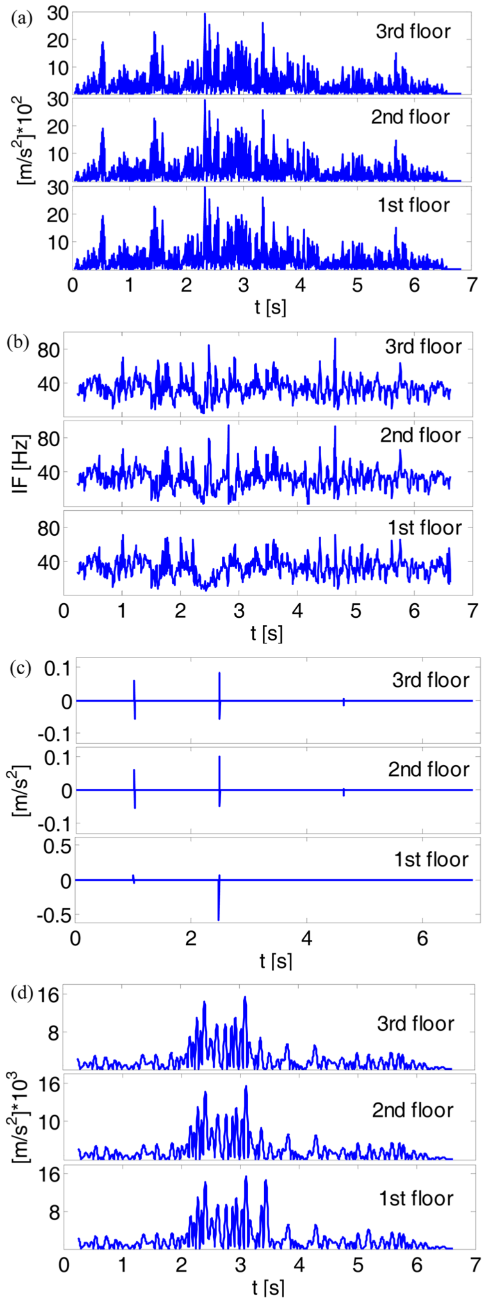

Fig. 15 Damage detection when the structure is exited by an acceleration record from the 1984 Round Valley earthquake: (a) First level detail functions (in absolute values) via DWT, (b) IF of the first IMF via HT, (c) IMF 1 with intermittency check at 100 Hz and (d) floor accelerations (in absolute values) after a 90 Hz high pass filter is applied

of the methodologies was capable of identifying all three damage instants at the three levels of the structure. The best results were obtained using the high pass filter at 90 Hz (Fig. 14(d)) and the DWT approach (Fig. 14(a)), where the three damage instants (at 5, 10 and 15 seconds) can be identified from the accelerations at the first level. The EMD methodology with an intermittency check at 100 Hz was able to detect only the larger induced damage (at 15 seconds) from the accelerations at the first level. No damage can be identified based on the IF of the first IMF (Fig. 14(b)).

The results obtained when the structure is excited by the Round Valley record are displayed in Fig. 15. The total duration of this record is 6.87 seconds, so spikes related to damage are expected around 1.72, 3.44 and 5.16 seconds. None of the 4 methodologies evaluated was able to clearly detect any damage instants from any of the floor accelerations. The results obtained using the EMD with intermittency check (Fig. 15(c)) show clear, isolated and congruent spikes in each of the floors; however the times of occurrence do not coincide with the times the damage was induced. The large amount of spikes obtained using the other three methodologies (Fig. 15(a), (b) and (d)) makes difficult an unambiguous identification of the damage instants.

5. Damage detection using the Continuous Wavelet Transform

It has been shown in the previous sections that signal processing based damage detection methodologies are successful when the system is excited by deterministic loads. However, problems arise when the system is excited by random loads like an earthquake. Since the detection of damage is based on the premise that its occurrence will be reflected in the high frequency component of the structural response, application of the available methodologies is limited by the frequency content of the load excitation. If the frequency content of the excitation spans over the frequency range where damage is reflected, the results obtained after a high frequency analysis may include not only spikes due to structural damage but also spikes proper of the excitation. To overcome this limitation an alternative approach using a projection of the structure high frequency response via the CWT instead of the DWT is proposed. Using the CWT has the advantage that the central frequencies at which it operates can be defined by the user (e.g., Montejo and Suarez 2007, Montejo and Kowalsky 2008), while the frequency bands of the detail functions obtained via DWT are predetermined by the sampling period of the signal. The procedure is exemplified using the first floor accelerations of the structure excited by the Round Valley earthquake. First, a redundant decomposition at high frequency levels of the excitation load and the first floor response is performed using the Complex Morlet Wavelet (Eq. (5)); the results are displayed in the WaveletMaps in Fig. 16(a) and (b), respectively. The decomposition was performed at every 1 Hz between 70 Hz and the Nyquist frequency (100 Hz). Notice that both maps are quite similar, which means that a large part of the structural response high frequency components arrive directly from the load excitation and are not related to damage. Nevertheless, a closer look to Fig. 16(b) can identify a dark vertical trend (around 3.4 seconds) that is not present on the excitation map (Fig. 16(a)) and which occurrence time coincide with one of the induce damage instants. In order to reduce the interference of the high frequency components proper of the base excitation on the analysis of the structural response, the ratio in absolute values of the wavelet coefficients from the first floor and base excitation is calculated. The results are displayed in Fig. 16(c), it is seen that all three damage instants become apparent. A more precise estimation of the damage instant can be obtained by

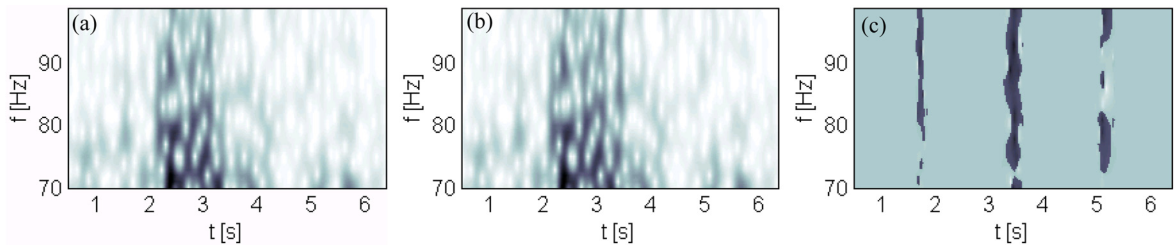

Fig. 16 High frequencies WaveletMaps of the load excitation – (a) Round Valley record and (b) the first floor dynamic response and (c) ratio of the Wavelet coefficients

finding the ratios maxima (points where the derivative with respect to time is zero) at each frequency. To avoid the identification of spurious peaks a threshold criterion is adopted, first the ratios (r) at each time instant (j) are normalized according to the rule:

$$z_j = \frac{r_j - \mu}{\sigma} \tag{10}$$

where μ and σ are the mean and the standard deviation of the ratio values. Any instant (j) where the normalized value (z) is larger than 2 (i.e., the ratio deviates more than 2 standard deviations from the mean value) is treated as a damage instant. The results obtained are shown in Fig. 17, it is seen that, with exception of the Round Valley earthquake case, the three damage instants can be detected for any of the other three excitations and at any of the structure levels. In the case of the Round Valley excitation, the 5% reduction in stiffness can only be detected from the first floor response (Fig. 17(d)).

It should be noticed that the first 4 methodologies (based on DWT, HHT, EMD and high pass filtering) were evaluated on an output-only fashion, that is, only the output signal (system response) was analyzed. However, in the case of the proposed CWT methodology, the input excitation is also required. To be fair on the evaluation of the other methods and explore if their performance is similarly improved when "ratios" to the input processed by their respective methods are implemented, the same type of analysis was carried out for the critical input excitation of the Round Valley earthquake for all four methodologies. The results are shown in Fig. 18. It is seen that in the case of the DWT, HHT and EMD based methodologies (Fig. 18(a), (b) and (c), respectively) the performance is not improved as a large number of spurious peaks not related to damage emerge. However, the high pass filtering methodology is significantly improved when the ratio of the high passed output to input signals is taken (Fig. 18(d)). It is seen that the results are comparable to the obtained with the CWT methodology (Fig. 17(d)) since all three levels of damage can be detected from the first floor response and the two largest ones can also be detected from the analysis of the second and third floor response. Nevertheless, some spurious spikes of significant amplitude appear around the damage instants that may complicate an unambiguous identification.

6. Conclusions

Four available methodologies for model-free signal-processing-based damage detection were examined using a three storey shear building subjected to different types of load. Damage is introduced as

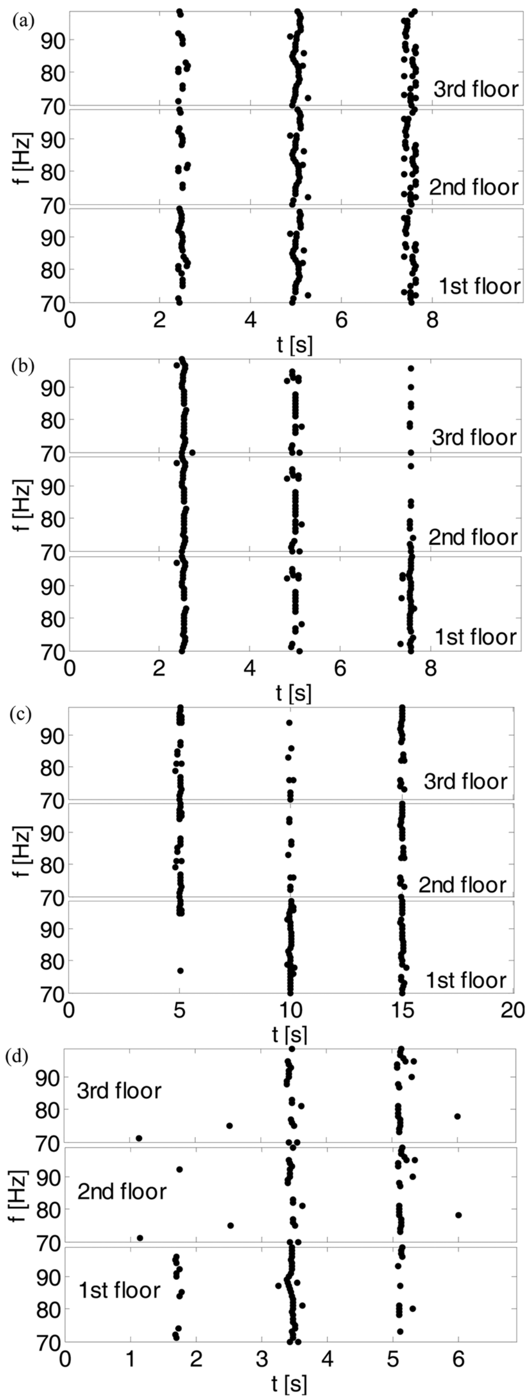

Fig. 17 Damage detection via CWT ratios for different excitations: (a) wnoise25; (b) wnoise40; (c) Loma Prieta record; (d) Round valley record

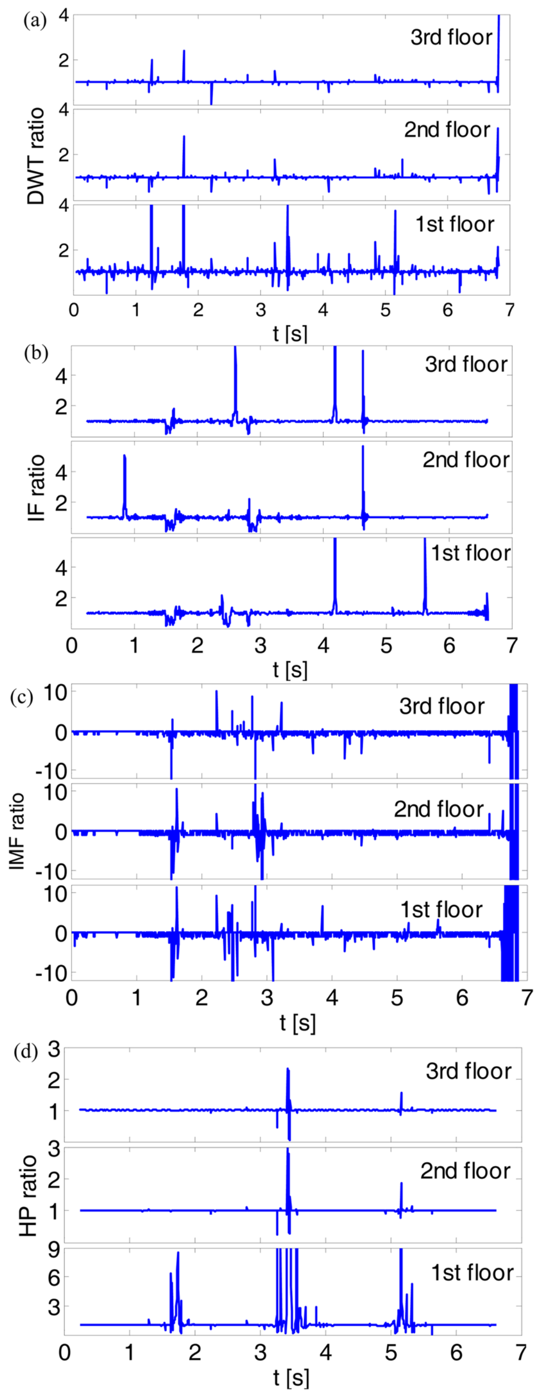

Fig. 18 Damage detection when the structure is exited by an acceleration record from the 1984 Round Valley earthquake using floor response to input motion ratios: (a) DWT ratio, (b) IF ratio, (c) IMF ratio and (d) high passed signals ratio

sudden relative reductions of 5%, 10% and 20% of the 1st floor stiffness. The methodologies examined are based on the detection of spikes on the high frequency response of the structure obtained via: (1) Discrete Wavelet Transform, (2) Hilbert Huang Transform, (3) Empirical Mode Decomposition with intermittency frequency and (4) Butterworth high pass filtering. It was found that successful unambiguous damage detection using such methods largely depends on the characteristics of the excitation load. Good results are obtained when the system is excited by deterministic loads. However, damage detection capabilities diminish as the system is excited by random loads and the high frequency content of the excitation increase. The best results were obtained using the high pass filtering technique.

A high frequency/highly redundant time-frequency analysis of the structural response and input excitation showed that a large part of the system response high frequency components may arrive directly from the load excitation and are not necessarily related to damage. An alternative approach based on a redundant decomposition of the structural response at high frequencies via the Continuous Wavelet Transform is then proposed. To reduce the effect of the input load high frequency content, damage instants are detected by the spikes resulting from the ratio between wavelet coefficients of the structural response and the excitation. The results obtained were quite promising as the three levels of induced damage were identified even when the input load has significant high frequency content. A similar output/input ratio approach was then implemented for the other four methodologies. Significant improvement was only noticed for the high pass filtering technique, though some spurious spikes of considerable amplitude emerged around the damage instant making difficult an

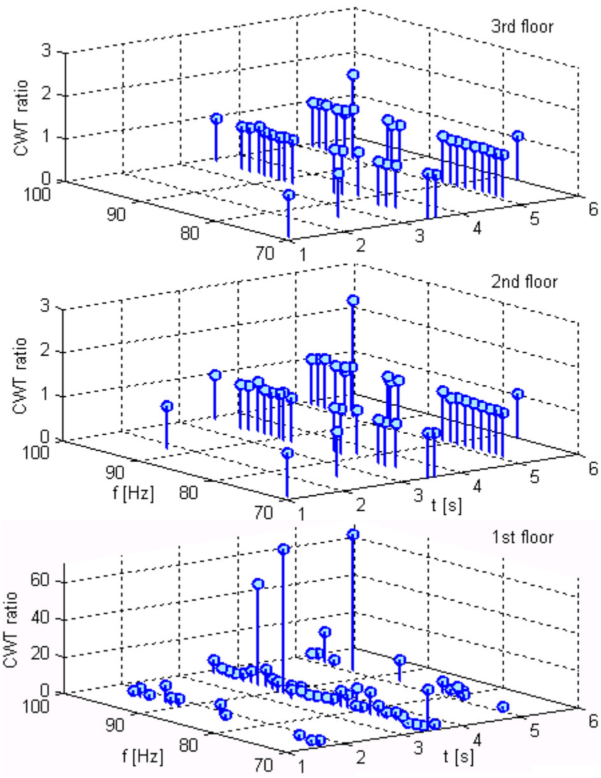

Fig. 19 3D stem plot showing ratio amplitudes for the CWT damage detection methodology (Round Valley excitation) explicit identification.

Identification of damage location and relative damage magnitude can be accomplished when the structure is excited by a stationary load with limited frequency content, e.g., the 3Hz constant amplitude sinusoidal signal used in this paper. It is seen, for example, that the spikes amplitude from the DWT details (Fig. 7) are larger in the first floor (where damage was induced) and increase as the level of damage increases. When the system is excited by a nonlinear-nonstationary load with wide frequency content, estimation of the relative level of damage is not evident from the results obtained. In Fig. 12(a) and 12(b) for example, the amplitude of the spikes do not correlate with the level of damage induced. This is because the spike amplitude not only depends on the level of damage but also on the external load and damage time. Nevertheless, identification of damage location is still viable as the larger spikes will be obtained on the measure points closer to the damage locations. This can be corroborated from Figs. 18(d) and 19, where the amplitude of the spikes emerging at the first floor is much larger than the spikes amplitude on the upper floors. Fig. 19 is a 3D version of Fig. 17(d) to show also the ratio value.

Finally, it should be noticed that a limitation of the proposed methodology is that input measurements are required and this is not always available in some monitoring applications (e.g., during operational monitoring under traffic, wind or other ambient loads when damage occurs under service loading). Further validation is required using data obtained from actual structures or more advance models (e.g., models that take into account soil structure interaction and have a more realistic approach for the simulation of damage). Notice that data gathered from actual structures is likely to have signal noise in the high frequency range where the applied signal processing techniques mainly work and new challenges may emerge.

References

Al-Khalidy, A., Noori, M., Hou, Z., Yamamoto, S., Masuda, A. and Sone, A. (1997), "Health monitoring systems of linear structures using wavelet analysis", *Proceeding of the 1st International Workshop on Structural Health Monitoring*, Stanford, CA.

Bisht, S.S. (2005), "Methods for structural health monitoring and damage detection of civil and mechanical systems", MS Thesis, Department of Engineering Science and Mechanics, Virginia Polytechnic Institute and State University.

Carmona, R.A., Hwang, W.L. and Torresani, B. (1997), "Characterization of signals by the ridges of their wavelet transforms", *IEEE T. Signal Proc.*, **54**(10), 2586-2590.

Clinton, J.F., Bradford, S.C., Heaton, T.H. and Favela, J. (2006), "The observed wander of the natural frequencies in a structure", *B. Seismol. Soc. Am.*, **96**(1), 237-257.

Doebling, S.W., Farrar, C.R., Prime, M.B. and Shevitz, D.W. (1996), *Damage identification and health monitoring of structural and mechanical systems from changes in their vibration characteristics: a literature review*, Los Alamos National Laboratory Report LA-13070-MS.

Doebling, S.W., Farrar, C.R. and Prime, M.B. (1998), "A summary review of vibration-based damage identification methods", *Shock Vib. Dig.*, **30**(2), 91-105.

EERI Earthquake Engineering Research Institute (2009), "Learning from earthquakes: The M6.3 Abruzzo, Italy, Earthquake of April 6, 2009", *EERI Special Earthquake Report*.

Farrar, C.R. and Cone, K.M. (1995), "Vibration testing of the 1-40 bridge before and after the introduction of damage", *Proceedings 73th international Modal Analysis Conference*, Nashville, TN.

Farrar, C.R., Doebling, S.W. and Nix DA. (2001), "Vibration based structural damage identification", *Philos. T. R. Soc. A*, **359**,131-149.

Hou, Z. and Noori, M. (1999), "Application of wavelet analysis for structural health monitoring", *Proceedings of* *the 2nd International Workshop on Structural Health Monitoring*, Stanford, CA.

Huang, N.E., Shen, Z., Long, S.R., Wu, M.C., Shih, H.H., Zheng, Q., Yen, N.C., Tung, C.C. and Liu, H.H. (1998), "The empirical mode decomposition and the Hilbert spectrum for nonlinear and non-stationary time series analysis", *Philos. T. R. Soc. A*, **454**, 903-995.

Huang, N.E., Shen, Z. and Long, S.R. (1999), "A new view of nonlinear water waves: the Hilbert spectrum", *Annu. Rev. Fluid Mech*., **31**, 417-457.

Huang, N.E. (2005), "Introduction to the Hilbert Huang transform and its related mathematical problems", *Hilbert Huang Transform and Its Applications*, World Scientific, 1-26.

Huth, O., Feltrin, G., Maeck, J., Kilic, N. and Motavalli, M. (2005), "Damage identification using modal data: experiences on a prestressed concrete bridge", *ASCE J. Struct. Eng.*, **131**(12), 1898-1910.

Kijewski, T. and Kareem, A. (2003), "Wavelets transforms for system identification in civil engineering", *Comput. Aided Civil Infra. Eng.*, **18**, 339-355.

Kijewski-Correa, T. and Kareem, A. (2006), "Efficacy of Hilbert and Wavelet transforms for time-frequency analysis", *J. Eng. Mech.*, **132**(10), 1037-1049.

Mallat, S.G. (1989), "Theory for multiresolution signal decomposition: the wavelet representation", *IEEE T. Pattern Anal.*, **11**(7), 674-693.

Montejo, L.A. and Kowalsky, M.J. (2008), "Estimation of frequency-dependent strong motion duration via wavelets and its influence on nonlinear seismic response", *Comput. Aided Civil Infra. Eng.*, **23**, 253-264.

Montejo, L.A. and Suarez, L.E. (2007), "Applications of the Wavelet Transform in structural engineering", *Mecánica Computacional*, **XXVI**, 2742-2753. (in Spanish)

Ovanesova, A.V. and Suarez, L.E. (2004), "Applications of wavelet transforms to damage detection of frame structures", *Eng. Struct.*, **26**, 39-49.

PEER Pacific Earthquake Engineering Research Center (2010), Next Generation Attenuation of Ground Motions NGA database. <http://peer.berkeley.edu/nga/index.html>

Rilling, G., Flandrin, P. and Gonçalvès, P. (2003), "On empirical mode decomposition and its algorithms", *IEEE-EURASIP Workshop on Nonlinear Signal and Image Processing NSIP-03*.

Rodgers, J.E. and Çelebi, M. (2006), "Seismic response and damage detection analyses of an instrumented steel moment-framed building", *ASCE J. Struct. Eng.*, **132**(10), 1543-1552.

Sohn, H., Farrar, C.R., Hemez, F.M., Shunk, D.D., Stinemates, D.W. and Nadler, B.R. (2003), *A review of structural health monitoring literature: 1996-2001*, Los Alamos National Laboratory Report LA-13976-MS.

Sone, A., Yamamoto, S., Nakaoka, A., Masuda, A. (1995), "Health monitoring system of structures based on orthonormal wavelet transform" *Proceedings of the ASME Pressure Vessels and Piping Conference*, 161-167.

Todorovska, M.I. (2001), "Estimation of instantaneous frequency of signals using the continuous wavelet transform," Report CE 01-07, Department of Civil Engineering, University of Southern California

Todorovska, M.I. and Trifunac, M.D. (2007), "Earthquake damage detection in the imperial county services building I: the data and time frequency analysis", *Soil Dyn. Earthq. Eng.*, **27**, 564-576.

Tododrovska, M.I. (2009), "Earthquake damage detection in buildings and early warning based on wave travel times", *Proceedings of 2009 NSF Engineering Research and Innovation Conference*, Honolulu, Hawaii.

Todorovska, M.I. and Trifunac, M.D. (2010), "Earthquake damage detection in the Imperial County Services building II: Analysis of novelties via wavelets", *Struct. Control Hlth. Monit.*, **17**(8), 895-917.

Vincent, H.T., Hu. S.J. and Hou, Z. (1999), "Damage detection using empirical mode decomposition and a comparison with wavelet analysis", *Proceedings of the 2nd International Workshop in Structural Health Monitoring*, Stanford, CA.

Xu, Y.L. and Chen, J. (2004) "Structural damage detection using empirical mode decomposition: experimental investigation", *J. Eng. Mech.*, **130**(11), 1279-1288.

Yan, B. and Miyamoto, A. (2006), "A comparative study of modal parameter identification based on Wavelet and Hilbert-Huang transforms", *Comput. Aided Civil Infra. Eng.*, **21**, 9-23.

Yang, J.N., Lei, Y., Lin, S. and Huang, N. (2004), "Hilbert-Huang based approach for structural damage detection", *J. Eng. Mech.*, **130**(1), 85-95.